Biomarker and therapeutic applications of a novel microRNA in early-stage knee osteoarthritis

Madhu Baghel PhD[1,2], Thomas G. Wilson BS[1,2], Trevor Banka MD[2], Jason Davis MD[3,4], Vasilios Moutzouros MD[2], Shabana Amanda Ali PhD[1,2,5,6*]

Affiliations: 1. Bone and Joint Center, Henry Ford Health + Michigan State University Health Sciences, Detroit, MI, USA; 2. Department of Orthopedic Surgery, Henry Ford Health, Detroit, MI, USA; 3. Michigan Orthopaedic Surgeons, West Bloomfield, MI, USA; 4. Department of Orthopaedic Surgery, Corewell Health William Beaumont University Hospital, Royal Oak, MI, USA; 5. Department of Physiology, Michigan State University, East Lansing, MI, USA; 6. Center for Molecular Medicine and Genetics, Wayne State University, Detroit, MI, USA

*Corresponding author:
Shabana Amanda Ali, PhD
Bone and Joint Center, Henry Ford Health, 6135 Woodward Avenue, Detroit MI 48202, USA
Email: sali14@hfhs.org

Abstract

Osteoarthritis is a debilitating joint disease with no known cure, underscoring the need for early detection and intervention. Given their potential disease-specificity, novel microRNAs are promising biomarkers and therapeutic targets. Novel microRNAs are identified from sequencing data using bioinformatics analyses. Here we aimed to characterize a novel microRNA (novel_miRNA_2; UCCCUGUUCGGGCGCCACU) in knee osteoarthritis. We show circulating novel_miRNA_2 accurately distinguishes early-stage knee osteoarthritis from both non-osteoarthritis and late-stage knee osteoarthritis. In knee osteoarthritis subchondral bone, novel_miRNA_2 functions as a canonical microRNA, downregulating target genes such as *RUNX2*. In male mice, novel_miRNA_2 mimic attenuates knee osteoarthritis when delivery begins in early stages, but not late stages. The decline in novel_miRNA_2 in late-stage knee osteoarthritis may be governed by Hedgehog signaling, which is known to upregulate genes such as *RUNX2* and exacerbate osteoarthritis. Our findings suggest endogenous novel_miRNA_2 can be used to detect early-stage knee osteoarthritis when exogenous delivery can mitigate disease.

Keywords

Arthritis, Early Diagnosis, Epigenetics, Targeted therapy

53 **Introduction**

54 Osteoarthritis (OA) is a debilitating joint disease currently impacting 7.6% of the global
55 population[1]. Most commonly affecting the knee[1], OA is characterized by phasic symptoms and
56 progressive joint damage, including articular cartilage degradation, synovial inflammation, and
57 subchondral bone remodeling[2]. There is no known cure for OA, and the molecular mechanisms
58 that drive OA pathogenesis are incompletely understood, particularly in early-stage disease when
59 prevention is still possible[3]. This points to a need for reliable biomarkers that can detect early-
60 stage OA and for effective therapeutics that can mitigate disease progression[4].

61

62 MicroRNAs are small non-coding RNAs with the potential to serve as both mechanistic
63 biomarkers and therapeutic targets in OA[5]. Functioning to repress gene expression via direct
64 binding to their target mRNAs[6], microRNAs regulate key biological processes in joint tissues[7]. As
65 biomarkers, circulating microRNAs are highly stable and can be linked to specific disease
66 contexts[8]. As therapeutics, microRNAs can be modulated using small molecules to either
67 enhance or inhibit their activity *in vivo* to mitigate disease processes[5,9]. Their dual function as
68 mechanistic biomarkers and therapeutic targets can link diagnosis to treatment, making
69 microRNAs strong candidates for precision medicine in OA.

70

71 Most studies to date have focused on established microRNAs that are cataloged in databases[10]
72 and characterized across different biological contexts[11]. In contrast, novel microRNAs are
73 sequences that are newly discovered through bioinformatics analyses of microRNA-sequencing
74 data[12]. Novel microRNAs align to the human reference genome, have a predicted hairpin
75 secondary structure typical of microRNA precursors, and lack homology with established
76 microRNAs in humans and other species[13]. With the potential to be completely unique to the
77 biological context in which they are discovered, novel microRNAs are ideal for first-in-class

microRNA biomarkers and therapeutics for OA. Despite their promise, the biological relevance and clinical utility of novel microRNAs in OA remains largely unknown.

In the first study to explore circulating novel microRNAs in OA, four candidates (novel_miRNA_1, novel_miRNA_2, novel_miRNA_3, and novel_miRNA_4) were found to be more prevalent in plasma from individuals with early- versus late-stage radiographic knee OA[14]. Here, we evaluate the biomarker potential of these four candidates in an independent patient cohort and prioritize novel_miRNA_2. Using both primary human knee OA tissues and a surgical mouse model of knee OA, we define expression profiles and therapeutic effects of novel_miRNA_2. Together, our findings suggest that novel_miRNA_2 is a promising biomarker for early-stage knee OA that functions as a canonical microRNA to prevent disease by repressing aberrant bone-related processes.

Results

Circulating novel_miRNA_2 distinguishes early-stage knee OA

Four novel microRNAs were previously reported in the plasma of individuals with early- versus late-stage radiographic knee OA[14] (**Figure 1A**). To validate these findings, we leveraged the Henry Ford Health (HFH) OA Cohort, a repository of human biofluids, tissues, and clinicodemographic data from individuals with symptomatic knee OA undergoing arthroscopy or arthroplasty. Participants were stratified by radiographic severity using the Kellgren-Lawrence (KL) grading system, with KL grade 0 or 1 defined as early-stage knee OA[15] and KL grade 3 or 4 as late-stage knee OA, consistent with previous definitions[14]. Non-OA plasma samples were obtained from the “Control Cohort” of the Osteoarthritis Initiative (OAI)[16] and included individuals with no symptomatic or radiographic evidence of knee OA.

104

105 Performing real-time PCR (RT-qPCR) using custom-designed TaqMan assays, no significant
106 differences were observed for novel_miRNA_1, novel_miRNA_3, or novel_miRNA_4
107 (**Supplemental Figure 1**), but novel_miRNA_2 was significantly elevated in early-stage knee OA
108 plasma compared to non-OA controls and late-stage knee OA (**Figure 1B**). When including KL
109 grade 2 samples, plasma levels of novel_miRNA_2 showed a significant inverse correlation with
110 KL grade (**Figure 1C**). Based on these findings, we evaluated the potential of novel_miRNA_2 to
111 distinguish early-stage knee OA using area under the receiver operating characteristic curve
112 analysis (AUC). Novel_miRNA_2 showed excellent accuracy in discriminating early-stage knee
113 OA from non-OA and good accuracy from late-stage knee OA (**Figure 1D**), as well as good
114 accuracy in distinguishing late-stage knee OA from non-OA (**Supplemental Figure 2**). Using
115 multivariable linear regression, we confirmed there were no associations between
116 novel_miRNA_2 plasma levels and age, sex, or body mass index (BMI), but significant
117 associations with early-stage knee OA (**Figure 1E**). Collectively, these findings prioritize
118 novel_miRNA_2 as a promising circulating biomarker for early-stage knee OA.

119

120 **Novel_miRNA_2 functions as a canonical microRNA**

121 Since novel_miRNA_2 was predicted to be a microRNA using only bioinformatics analyses[14], we
122 aimed to experimentally verify its authenticity based on known properties of canonical
123 microRNAs[6]. MicroRNA biogenesis begins with transcription of a primary ("pri-") transcript from a
124 host gene, which folds into a hairpin structure[6]. This precursor undergoes enzymatic cleavages
125 to generate mature microRNAs that are loaded into Argonaute 2 (AGO2)-containing RNA-induced
126 silencing complexes (RISCs) to mediate repression of target genes[6] (**Figure 2A**). Prior to
127 experimentation, we aligned the predicted novel_miRNA_2 precursor to the human reference
128 genome (GRCh38) and identified its host gene as Zinc Finger Protein 773 (*ZNF773*), with
129 novel_miRNA_2 located on the reverse strand (**Figure 2B**). We also identified the mature

130 novel_miRNA_2 sequence on the 5' arm of the precursor molecule, which designates it as a "-
131 5p" microRNA by standard conventions[17] (**Figure 2B**).
132
133 We leveraged the steps of microRNA biogenesis to identify the knee OA tissues that express
134 novel_miRNA_2. Specifically, we quantified *ZNF773*, pri-novel_miRNA_2, and mature
135 novel_miRNA_2 in subchondral bone, infrapatellar fat pad ("fat pad"), articular cartilage, and
136 synovium using RT-qPCR. In early- versus late-stage knee OA tissues, *ZNF773* was significantly
137 higher in subchondral bone, fat pad, and synovium (**Figure 2C**), pri-novel_miRNA_2 was higher
138 in subchondral bone and fat pad (**Figure 2D**), and mature novel_miRNA_2 was higher in
139 subchondral bone, fat pad, synovium, and articular cartilage (**Figure 2E**). Since the mature form
140 is derived from the primary transcript, we performed correlation analyses between mature
141 novel_miRNA_2 and pri-novel_miRNA_2 levels and found significant positive associations in
142 subchondral bone ($n = 14$, $R = 0.69$, $p = 0.01$) and fat pad ($n = 14$, $R = 0.67$, $p = 0.01$). To assess
143 incorporation of novel_miRNA_2 into RISCs, we performed an AGO2-RNA immunoprecipitation
144 assay in human knee OA subchondral bone (**Figure 2F**). We found significant enrichment of
145 novel_miRNA_2 in AGO2-bound fractions compared with IgG fractions, while there was no
146 enrichment of negative control U6 small nuclear RNA (**Figure 2G**). Taken together, these results
147 show that novel_miRNA_2 is elevated in early- versus late-stage knee OA tissues and follows
148 canonical microRNA biogenesis most consistently in subchondral bone.
149
150 **Novel_miRNA_2 inhibits target genes in knee OA subchondral bone**
151 To elucidate molecular mechanisms of novel_miRNA_2 in knee OA, we sought to identify its direct
152 target genes. MicroRNAs inhibit gene expression through complementary seed-sequence
153 binding, most often within the 3' untranslated region (UTR) of a target mRNA[6]. Using an *in silico*
154 approach[18], we first identified 2,951 human genes that contained at least one putative 7mer or
155 8mer novel_miRNA_2 seed-sequence binding site in their 3' UTR (**Figure 3A**). Second, we

156 evaluated binding site stability by calculating the Gibbs free energy (ΔG) for the 70-nucleotide
157 flanking regions of each binding site, comparing them with 3' UTR-wide averages. Sites with
158 greater than average flanking ΔG were retained, indicative of less stable mRNA secondary
159 structures and higher accessibility for RISC binding[19], resulting in 1,463 genes (**Figure 3A**). Third,
160 to focus on OA, we cross-referenced this list with bone-related datasets curated in OsteoDIP[20],
161 leaving 87 genes (**Figure 3A**). Finally, we performed pathway analysis[21] on this subset and found
162 enrichment of curated 'Diseases and Functions' and 'Canonical Pathways' that relate to OA
163 (**Supplemental Figure 3**), resulting in a final shortlist of 13 candidate target genes (**Figure 3B**).
164
165 To validate these predicted targets, we transfected human knee OA subchondral bone explants
166 with a custom-designed novel_miRNA_2 mimic to enhance its levels and then assessed
167 expression of the 13 genes (**Figure 3C**). Nine genes (*ASPN*, *RUNX2*, *ATRNL1*, *ADRA2A*,
168 *SLC2A4*, *ITGA11*, *IL11*, *ALPL*, and *MMP25*) were significantly downregulated with
169 novel_miRNA_2 mimic treatment versus negative control treatment, and four genes (*APOD*,
170 *PARD6G*, *ADIPOQ,* and *LEP*) were not significantly different (**Figure 3C**). These results are
171 consistent with the expected inhibitory effect of microRNAs on their direct target genes[6]. To
172 assess functional effects of novel_miRNA_2 in subchondral bone, we explored bone
173 mineralization, a process required for the osteophyte formation and subchondral sclerosis
174 observed in OA[22]. In murine pre-osteoblast cells transfected with novel_miRNA_2 mimic**,** there
175 was a significant reduction in mineral deposition compared to negative control (**Figure 3D, E**).
176 Together, these results suggest that novel_miRNA_2 functions to regulate target genes and bone-
177 related processes such as mineralization in knee OA subchondral bone.
178
179 **Novel_miRNA_2 has a protective effect in early-stage knee OA**
180 To assess the effect of novel_miRNA_2 on knee OA *in vivo*, we leveraged the partial medial
181 meniscectomy (PMX) mouse model[23]. Since species specificity was a criterion used to discover

182 novel_miRNA_2, it is predicted to occur in humans but not mice[13,14]. Consistent with this, we found
183 no matching sites upon aligning either the precursor or mature novel_miRNA_2 sequences to the
184 mouse reference genome (GRCm39). We were therefore able to precisely control
185 novel_miRNA_2 levels in mice using mimic treatments. Based on our data showing
186 novel_miRNA_2 is elevated in circulation during early-stage knee OA (**Figure 1B**), and previous
187 literature characterizing OA pathology in PMX mice over time[24], we compared intravenous
188 treatment beginning at two different timepoints (**Figure 4A**). Early treatment began one week
189 post-operatively, when cartilage degradation, osteophyte formation, and synovitis are all
190 underway, while late treatment began four weeks post-operatively, when these processes are
191 more established[24] (**Figure 4A**). To first confirm that the novel_miRNA_2 mimic was reaching
192 knee tissues following intravenous delivery, we performed *in situ* hybridization and observed a
193 positive signal in the subchondral bone of mimic-treated mice one week post-surgery compared
194 to negative control treatment (**Figure 4B**). Notably, signal intensity was greater in PMX knees
195 compared to sham knees (**Figure 4B**), suggesting that circulating novel_miRNA_2 accumulates
196 in mouse tissues during knee OA, as observed in human tissues (**Figure 2E**).
197
198 To assess knee OA severity, we evaluated cartilage degradation, osteophyte burden, and
199 synovitis as well-characterized features in the PMX model[24]. Compared to negative control
200 treatment, we found novel_miRNA_2 mimic reduced cartilage degradation (**Figure 4C, D**) and
201 osteophyte burden (**Figure 4E, F**) in PMX knees, but only when treatments began at earlier stages
202 and not later stages. No significant effect on synovitis was observed with either treatment strategy
203 (**Supplemental Figure 4**). These findings suggest novel_miRNA_2 likely functions to mitigate
204 tissue-specific disease processes in early stages of OA, but cannot reverse those processes once
205 established in later stages.
206
207 **Hedgehog signaling may regulate novel_miRNA_2 levels in knee OA**

208 Given the disease stage-dependent biomarker (**Figure 1**) and therapeutic (**Figure 4**) patterns
209 exhibited by novel_miRNA_2, we sought to identify upstream factors governing its levels in early-
210 versus late-stage knee OA. Taking an *in silico* approach to identifying transcription factor binding
211 sites within the promoter region of the *ZNF773* host gene, we found three GLI consensus binding
212 motifs located within 2.5 kb of novel_miRNA_2 (**Figure 5A**). GLI transcription factors are the
213 primary effectors of the Hedgehog (Hh) signaling pathway, which is known to exacerbate knee
214 OA[25]. Since Hh signaling upregulates Runt Related Transcription Factor 2 (*RUNX2)*[25], a regulator
215 of bone formation[26] and a predicted target gene of novel_miRNA_2 (**Figure 3B, C**), we
216 hypothesized that Hh signaling governs novel_miRNA_2 levels in knee OA subchondral bone.
217
218 To investigate Hh signaling in early- versus late-stage human knee OA subchondral bone, we
219 measured the Hh target genes GLI Family Zinc Finger 1 (*GLI1*), Patched 1 (*PTCH1*), and
220 Hedgehog Interacting Protein (*HHIP*) as markers of pathway activity[25,27]. All three targets were
221 lower in early- versus late-stage knee OA subchondral bone, as were levels of *RUNX2* (**Figure**
222 **5B**), consistent with the positive relationship previously reported between Hh signaling and
223 *RUNX2* levels[25]. Together with the higher levels of *ZNF773*, pri-novel_miRNA_2, and mature
224 novel_miRNA_2 we observed in early-stage knee OA subchondral bone (**Figure 2C-E**), these
225 findings point to an inverse relationship between Hh signaling and novel_miRNA_2.
226
227 To assess the extent to which Hh signaling regulates novel_miRNA_2 levels, we treated human
228 knee OA subchondral bone explants with the Hh agonist purmorphamine[28] or vehicle control
229 (**Figure 5C**). Hh pathway activation by purmorphamine was confirmed by an increase in *GLI1*,
230 *PTCH1*, and *HHIP* compared to vehicle control (**Figure 5D**). Concurrently, we observed
231 significant reductions in *ZNF773*, pri-novel_miRNA_2, and mature novel_miRNA_2, along with
232 increased expression of *RUNX2* (**Figure 5D**). These findings suggest that Hh signaling can

233 reduce novel_miRNA_2 and remove the inhibitory effect novel_miRNA_2 has on target genes
234 such as *RUNX2.* Consistent with this, when novel_miRNA_2 levels were restored via mimic
235 treatment (**Figure 5C**), *RUNX2* expression decreased, even in the presence of Hh agonist
236 (**Figure 5E**). Taken together, these findings suggest that Hh signaling may govern the decline in
237 novel_miRNA_2 levels from early- to late-stage knee OA, and when restored, novel_miRNA_2
238 can mitigate the effect of Hh signaling on *RUNX2* in knee OA subchondral bone (**Figure 6**).
239
240
241 **Discussion**
242 Here we characterize a novel microRNA with the potential to be unique to OA. The
243 novel_miRNA_2 sequence has been reported by two studies profiling circulating novel
244 microRNAs in OA[14,29], but has not been reported in other studies profiling novel microRNAs in
245 non-OA human biospecimens[12,30,31]. We show circulating novel_miRNA_2 can distinguish early-
246 stage knee OA from both non-OA controls and late-stage knee OA, suggesting utility as a
247 minimally invasive biomarker. In human knee OA subchondral bone, novel_miRNA_2 functions
248 as a canonical microRNA that is transcribed from the *ZNF773* host gene, processed from primary
249 transcript into mature form, and incorporated into AGO2-containing RISCs to inhibit putative direct
250 target genes such as *RUNX2*. In a preclinical model, novel_miRNA_2 mimic reduces osteophyte
251 burden and cartilage degradation when administered beginning in early, but not later stages of
252 knee OA, suggesting it has a preventative effect but not a restorative effect. The decline in
253 novel_miRNA_2 levels from early- to late-stage disease may be regulated in part by Hh signaling,
254 which becomes activated in later stages of knee OA and upregulates *RUNX2*, potentially by
255 inhibiting novel_miRNA_2. To our knowledge, this study is the first comprehensive
256 characterization of a circulating novel microRNA in OA.
257

258 Reliable biomarkers for early-stage knee OA can transform clinical care by identifying patients for
259 first-line interventions before irreversible joint damage has occurred. While serum biomarkers
260 such as cartilage oligomeric matrix protein[32] and matrix metallopeptidase 3[33] have been explored
261 in early-stage knee OA, these are not yet in clinical use and are subject to challenges associated
262 with protein biomarkers[34]. MicroRNA biomarkers have been explored in knee OA[35] and other
263 musculoskeletal diseases[36], but novel microRNAs offer unique advantages. Novel microRNAs
264 may confer greater specificity and sensitivity as biomarkers since they are considered to be less
265 evolutionarily conserved than established microRNAs, often displaying species-specific or
266 lineage-restricted expression patterns[12,31]. Here, we show circulating novel_miRNA_2 in early-
267 stage knee OA can distinguish both the presence of OA and stage of OA[37], suggesting it has
268 potential as a diagnostic biomarker. Though not explored in the current study, novel_miRNA_2
269 may also have potential as a prognostic biomarker[37], where patients with higher levels of
270 novel_miRNA_2 or longer exposure to novel_miRNA_2 experience slower rates of OA
271 progression. This biomarker potential, together with its protective effects on knee OA, position
272 novel_miRNA_2 as a promising candidate for precision medicine linking patient stratification to
273 targeted interventions, where endogenous novel_miRNA_2 can be used to detect early-stage
274 knee OA and exogenous supplementation can mitigate disease progression.
275
276 Our data show novel_miRNA_2 functions as a canonical microRNA in human knee OA
277 subchondral bone and reduces osteophyte burden in mice with knee OA, suggesting it regulates
278 bone-related processes. Structural changes in bone are commonly observed in OA[38] and can
279 have negative effects on surrounding tissues[39], including cartilage[40]. As such, preventing
280 abnormal bone-related processes in early-stage knee OA via novel_miRNA_2 offers a viable
281 therapeutic strategy. It remains unknown if novel_miRNA_2 reduces cartilage damage indirectly,
282 via changes in bone, or more directly, via regulation of cartilage-related target genes, but available
283 evidence suggests the former. In early-stage knee OA cartilage, the trends towards elevated

284 novel_miRNA_2 biogenesis we observed were not significant. Consistent with this, a study
285 profiling novel microRNAs in human osteoarthritic chondrocytes did not report the
286 novel_miRNA_2 sequence[41], though this may be due to the study design. Meanwhile in early-
287 stage knee OA fat pad, we show novel_miRNA_2 biogenesis is elevated. The fat-related target
288 genes we predicted did not show significant differences with novel_miRNA_2 modulation in
289 subchondral bone, but they may be regulated by novel_miRNA_2 in fat pad, as microRNAs are
290 known to have tissue-specific effects[42]. In support of tissue specificity, novel_miRNA_2 had no
291 effect on synovitis in mice with knee OA, and therefore is unlikely to act on synovium. In this study
292 we prioritized bone-related genes previously implicated in OA, yet we predicted nearly 3,000
293 direct targets of novel_miRNA_2. Thus, there is a need to elucidate the network of
294 novel_miRNA_2 target genes within and across joint tissues to understand its role in OA, including
295 in regulating entirely new disease mechanisms.
296
297 The biomarker and therapeutic potential exhibited by novel_miRNA_2 specifically in early-stage
298 knee OA led us to investigate factors governing this stage-dependent activity. Given our focus on
299 subchondral bone and the presence of GLI consensus binding motifs upstream of
300 novel_miRNA_2, we explored Hh signaling, which is known to upregulate *RUNX2* and exacerbate
301 OA in late stages[25]. We hypothesize the lack of Hh signal in early-stage knee OA allows
302 novel_miRNA_2 biogenesis to proceed and inhibit *RUNX2*, while the presence of Hh signal in
303 late-stage knee OA reduces novel_miRNA_2 via GLI repressor isoforms[43], leaving target genes
304 such as *RUNX2* unchecked and promoting aberrant bone-related processes. Under this
305 hypothesis, sustaining novel_miRNA_2 levels from early- to late-stage knee OA is a strategy to
306 mitigate the effects of Hh signaling. This approach may be preferred over inhibition of Hh
307 signaling, which can have off-target effects[44]. Further research is needed to define parameters
308 such as the optimal treatment window for use of novel_miRNA_2 as a therapeutic in knee OA.
309

310 To note limitations of this study, validation in larger, independent cohorts is required to assess
311 the generalizability and clinical utility of novel_miRNA_2 as a diagnostic or prognostic biomarker.
312 Additionally, while *in silico* analyses were used to predict direct target genes of novel_miRNA_2,
313 transcriptional regulation must be verified through reporter construct assays, and indirect target
314 genes must be considered. Finally, we do not perform intra-articular delivery of novel_miRNA_2
315 mimic to target the local joint environment in mice. However, we show intravenous delivery of
316 mimic leads to localization in mouse knee OA tissues, which can be considered a less invasive
317 treatment approach that is amenable to future clinical translation[45].
318
319 In conclusion, this study demonstrates the potential of novel microRNAs to serve as biomarkers
320 and therapeutic targets in complex diseases. We show novel_miRNA_2 is associated with early-
321 stage knee OA, functioning as a canonical microRNA in subchondral bone to mitigate bone-
322 related processes. With further development, this microRNA could support precision medicine
323 approaches in OA care, being used as a biomarker to identify early-stage knee OA patients and
324 a therapeutic to prevent disease progression by targeting tissue-specific mechanisms.
325
326
327 **Methods**
328
329 **Ethical approval and study cohort**
330 Early- and late-stage knee OA biospecimens were obtained from the HFH OA Cohort. Assessed
331 by an orthopedic surgeon, the early-stage knee OA group comprised symptomatic individuals
332 undergoing knee arthroscopy with KL grade 0 or 1[15,29], and the late-stage knee OA group
333 comprised symptomatic individuals undergoing total knee arthroplasty with KL grade 3 or 4[14].
334 Non-OA plasma samples were obtained from the Osteoarthritis Initiative (OAI) “Control Cohort”,
335 comprising individuals without knee symptoms, radiographic knee OA, or risk factors for OA.

336 Further details about the OAI are available at: https://nda.nih.gov/oai[16]. Clinicodemographic
337 variables, including age, self-reported sex, BMI, race, and comorbidities were collected and de-
338 identified for all participants (**Supplemental Table 1**). Ethical approval was obtained from the
339 HFH Institutional Review Board (IRB #13995) for the HFH OA Cohort and via the University of
340 California, San Francisco (FWA approval #00000068; IRB approval #10-00532) for the OAI. All
341 methods were performed following the Declaration of Helsinki guidelines[46].
342
343 Briefly, whole blood samples were centrifuged at 3200 x g for 10 minutes at 4°C to obtain plasma.
344 Early- and late-stage knee OA tissues were collected and processed using our published
345 protocols[47] and included subchondral bone, infrapatellar fat pad, articular cartilage, and synovium.
346 Tissues were collected intraoperatively and dissected under sterile conditions within four hours of
347 surgery. Biospecimens were either used immediately after processing or flash frozen in liquid
348 nitrogen and stored at -80°C until use.
349
350 **Real-time quantitative polymerase chain reaction (RT-qPCR)**
351 For plasma, RNA was isolated using the miRNeasy Serum/Plasma Advanced Kit (QIAGEN)
352 according to the manufacturer's instructions. For tissue explants, RNA was extracted following
353 our published protocols[47]. Briefly, this included tissue homogenization in TRIzol reagent
354 (Thermofisher Scientific) followed by two rounds of chloroform extraction, then precipitation with
355 100% isopropanol. Pellets were washed with ice-cold 75% ethanol, air-dried, and eluted in
356 nuclease-free water. RNA quality and concentration were determined using a NanoDrop 2000
357 spectrophotometer (Thermofisher Scientific).
358
359 For microRNA quantification, reverse transcription was performed using the TaqMan microRNA
360 Reverse Transcription Kit (Applied Biosystems) with custom TaqMan Small RNA assays (Applied
361 Biosystems). For gene expression analyses, cDNA was synthesized using the High-Capacity

362 cDNA Reverse Transcription Kit (Applied Biosystems). RT-qPCR was performed using a
363 QuantStudio 7 Pro system (Applied Biosystems) with TaqMan Small RNA/Gene Expression
364 Assays (Applied Biosystems) or SYBR Green-based DNA oligonucleotides (Sigma-Aldrich). A list
365 of probes and primers is provided in **Supplemental Table 2**. MiR-24-3p and *GAPDH* were used
366 as internal reference controls for microRNA and gene analyses, respectively, as done previously[8].
367 Relative expression levels were calculated using the delta-delta-Ct method[48].
368

369 **Novel_miRNA_2 mimic transfection**

370 A custom miRIDIAN microRNA mimic (Dharmacon) corresponding to the novel_miRNA_2
371 sequence (UCCCUGUUCGGGCGCCACU) was designed for use both *in vitro* and *in vivo*. This
372 synthetic double-stranded RNA oligonucleotide comprised the mature novel_miRNA_2 sequence
373 and its complement, with chemical enhancements to preferentially select the mature
374 novel_miRNA_2 sequence for loading into RISCs. Mimic specificity was confirmed by RT-qPCR
375 standard curve analysis. Primary human subchondral bone explants (~100 mg/well) were
376 transfected in 24-well plates with 100 nM novel_miRNA_2 mimic or miRIDIAN Human Negative
377 Control Mimic ("negative control"). Transfection was performed using DharmaFECT-1
378 (Dharmacon) transfection reagent in 500 µL/well serum-free Dulbecco's Modified Eagle's Medium
379 (DMEM) supplemented with 1% penicillin-streptomycin (pen-strep, Gibco). To induce Hh pathway
380 activity with an agonist, explants were treated with 10 µM purmorphamine[28] (APExBio) or dimethyl
381 sulfoxide (DMSO) vehicle for 24 hours, with a subset concurrently transfected with 100 nM
382 novel_miRNA_2 mimic.
383

384 **Bioinformatics**

385 Novel_miRNA_2 target genes were predicted by complementary alignment of its seed-sequence
386 (nucleotide position 2-8) to the 3' UTRs of all human transcripts annotated in Ensembl BioMart
387 (GRCh38). Putative 8mer, 7mer-m8, and 7mer-A1 matches were retained for further analysis as

388 these binding site configurations are recognized as the strongest and most efficient for microRNA-
389 mediated gene repression[49]. Genes were further assessed for microRNA accessibility by
390 computing the minimum free energy of the 70-nucleotide regions upstream and downstream of
391 the seed-sequence binding sites using RNAfold (ViennaRNA package, v.2.5.1)[50]. The mean
392 flanking region delta Gibbs free energy (ΔG) was compared to the average ΔG of all other 70-
393 nucleotide windows within the same 3' UTR; binding sites with mean flanking region ΔG above
394 the global 3' UTR average were prioritized[19]. To select target genes most relevant to OA
395 subchondral bone, genes were cross-referenced with the OsteoDIP database
396 (https://ophid.utoronto.ca/OsteoDIP)[20], filtering for studies conducted in "subchondral bone",
397 "femoral condyles", "medial and lateral tibial plateaus", and "proximal femur". Pathway core
398 analysis was performed using Ingenuity Pathway Analysis software (QIAGEN)[21]. Putative
399 transcription factor binding sites within the promoter region of *ZNF773* (transcript
400 NM_001304334.2) were identified using the JASPAR (https://jaspar.elixir.no/)[51] transcription
401 factor motif database.
402
403 **AGO2-RNA immunoprecipitation**
404 AGO2-RNA immunoprecipitation experiments were adapted from an established protocol[52].
405 Briefly, 100 mg primary human knee OA subchondral bone was lysed in NP40 buffer with protease
406 and RNase inhibitors. After pre-clearing, 200 µL lysate was incubated with 3 µg of anti-AGO2 or
407 IgG antibodies bound to pre-blocked Dynabeads™ Protein G (Thermofisher Scientific). IgG was
408 used as a control for the detection of non-specific protein binding. AGO2/IgG complexes were
409 washed and RNA was extracted using our published protocols[47]. RT-qPCR analysis was
410 performed to measure novel_miRNA_2 and U6 small nuclear RNA levels in AGO2- and IgG-
411 bound fractions. U6 small nuclear RNA was used as a non-microRNA control that does not
412 associate with RISCs and therefore should not co-precipitate with AGO2[52].
413

414 **Cell mineralization assay**

415 Murine MC3T3-E1 pre-osteoblasts were seeded in 12-well plates at 6.0×10^4 cells/mL and
416 cultured at 37°C (with 5% CO_2) in Minimum Essential Medium Alpha (α-MEM) supplemented with
417 10% fetal bovine serum and 1% pen-strep. At 80% confluence, cells were supplemented with 10
418 mM β-glycerophosphate and 50 µg/mL ascorbic acid-2-phosphate to induce differentiation.
419 Simultaneously, the cells were treated with 20 nM novel_miRNA_2 mimic or negative control.
420 After 21 days of culture, cells were fixed in 10% neutral buffered formalin (NBF) and mineralization
421 was assessed by von Kossa[53] and Alizarin Red S (ARS) staining[54] using established protocols.
422 Briefly, for von Kossa, fixed cells were stained with 1% aqueous silver nitrate under ultraviolet
423 light, and unreacted silver was neutralized with 5% sodium thiosulfate. For ARS, fixed cells were
424 stained with 2% ARS (Sigma-Aldrich), then washed thoroughly. Images were captured at 2x
425 magnification using an Eclipse Ti microscope (Nikon). Bound ARS dye was extracted using 10%
426 acetic acid and average absorbance across technical replicates measured at 405 nm using a
427 plate reader (Perkin-Elmer).

428

429 **Animal experiments**

430 Male C57BL/6J mice at 11 weeks of age were purchased from Jackson Laboratories and
431 acclimatized for one week prior to surgery. All animals were housed under a 12-hour light/dark
432 cycle at 21°C and 30% humidity. Animals were handled by trained personnel and closely
433 monitored for signs of distress for the duration of the experiments to minimize suffering. Knee OA
434 was induced at 12 week of age using the partial medial meniscectomy (PMX) model as previously
435 described[8], with a concurrent group of mice undergoing sham surgery. Animals were randomized
436 into treatment groups comprising tail vein injections of 5 µg (in 50 µL 1X PBS) novel_miRNA_2
437 mimic or negative control delivered weekly according to the regimens shown in **Figure 4A**. At
438 endpoint (8 weeks post-surgery), animals were euthanized via CO_2 asphyxiation with cervical

439 dislocation secondary assurance of death, and hind limbs were harvested. Animal experiments
440 were approved by the HFH Institutional Animal Care and Use Committee (IACUC #1616).
441
442 **Histological analyses**
443 Mouse knee joints were fixed in 10% NBF at room temperature for 4 days followed by
444 decalcification using a 20% ethylenediaminetetraacetic acid (EDTA) solution for 21 days.
445 Samples were paraffin-embedded, coronally sectioned at 5-micron thickness onto charged slides,
446 then deparaffinized and stained with 0.1% Safranin-O. Cartilage damage was assessed using
447 OARSI scoring[55]. Joints were divided into medial and lateral tibial/femoral quadrants and graded
448 from 0 (no cartilage damage) to 6 (>75% cartilage thickness loss) by two independent blinded
449 observers, with the mean maximal quadrant score assigned to each sample. Synovitis was
450 assessed using the Krenn scoring system[56]. Values from 0 (normal) to 3 (severe) were assigned
451 for each of synovial lining thickness, stromal cell density, and inflammatory infiltration, then
452 summed for a maximum score of 9. For osteophytes, cross-sectional areas were manually drawn
453 and areas for the medial tibia and medial femur were quantified and averaged[57].
454
455 To assess novel_miRNA_2 mimic localization via *in situ* hybridization, mouse knee joints were
456 fixed and decalcified as described above. Tissues were then sectioned onto charged RNAse-free
457 slides at 2-micron thickness. Signal was visualized using a custom-designed novel_miRNA_2
458 miRNAScope probe (Advanced Cell Diagnostics) with the RNAScope 2.5 HD Kit, according to the
459 manufacturer's instructions.
460
461 **Statistical analyses**
462 All data analyses were performed using R 4.2.0 statistical software; specific R packages are
463 available upon request. Unless otherwise noted, all datapoints represent biological replicates. For
464 all experiments, normality was assessed using the Shapiro-Wilk test. For comparisons across

465 three or more groups, statistical significance was determined by one-way analysis of variance
466 (ANOVA) followed by Tukey's HSD post hoc test or the Kruskal-Wallis test followed by Dunn's
467 post hoc test. For comparisons between two groups, statistical significance was determined by
468 two-sided unpaired Welch's T-test, paired Student's T-test, or Mann-Whitney U-test. Pearson
469 correlation was performed between novel_miRNA_2 levels and KL grade. Multiple linear
470 regression analysis was used to assess associations with covariates. AUCs were generated using
471 the pROC v.1.18.5 R package.
472
473
474
475
476
477
478
479
480
481
482
483
484
485
486
487
488
489
490

491 **References**

492 1. Steinmetz, J.D.*, et al.* Global, regional, and national burden of osteoarthritis, 1990–2020
493 and projections to 2050: a systematic analysis for the Global Burden of Disease Study
494 2021. *The Lancet Rheumatology* **5**, e508-e522 (2023).

495 2. Dieppe, P.A. & Lohmander, L.S. Pathogenesis and management of pain in osteoarthritis.
496 *The Lancet* **365**, 965-973 (2005).

497 3. Felson, D.T. & Hodgson, R. Identifying and treating preclinical and early osteoarthritis.
498 *Rheum Dis Clin North Am* **40**, 699-710 (2014).

499 4. Kaushik, A.*, et al.* Advancing osteoarthritis management: integrating new insights and
500 addressing persistent roadblocks. *Inflammopharmacology*, 1-14 (2025).

501 5. Ali, S.A., Peffers, M.J., Ormseth, M.J., Jurisica, I. & Kapoor, M. The non-coding RNA
502 interactome in joint health and disease. *Nature Reviews Rheumatology* **17**, 692-705
503 (2021).

504 6. Shang, R., Lee, S., Senavirathne, G. & Lai, E.C. microRNAs in action: biogenesis, function
505 and regulation. *Nature Reviews Genetics* **24**, 816-833 (2023).

506 7. Szala, D.*, et al.* The Role of MicroRNAs in the Pathophysiology of Osteoarthritis. *Int J Mol*
507 *Sci* **25**(2024).

508 8. Wilson, T.G.*, et al.* Circulating miR-126-3p is a mechanistic biomarker for knee
509 osteoarthritis. *Nature Communications* **16**, 2021 (2025).

510 9. Wilson, T.G., Baghel, M. & Ali, S.A. Osteoarthritis year in review 2025: Genetics,
511 genomics, and epigenetics. *Osteoarthritis Cartilage* (2025).

512 10. Griffiths-Jones, S., Grocock, R.J., van Dongen, S., Bateman, A. & Enright, A.J. miRBase:
513 microRNA sequences, targets and gene nomenclature. *Nucleic Acids Res* **34**, D140-144
514 (2006).

515 11. Nalbant, E. & Akkaya-Ulum, Y.Z. Exploring regulatory mechanisms on miRNAs and their
516 implications in inflammation-related diseases. *Clin Exp Med* **24**, 142 (2024).

517 12. Friedländer, M.R.*, et al.* Evidence for the biogenesis of more than 1,000 novel human
518 microRNAs. *Genome Biol* **15**, R57 (2014).
519 13. Potla, P., Ali, S.A. & Kapoor, M. A bioinformatics approach to microRNA-sequencing
520 analysis. *Osteoarthritis and Cartilage Open* **3**, 100131 (2021).
521 14. Ali, S.A.*, et al.* Sequencing identifies a distinct signature of circulating microRNAs in early
522 radiographic knee osteoarthritis. *Osteoarthritis and Cartilage* **28**, 1471-1481 (2020).
523 15. Luyten, F.P.*, et al.* Toward classification criteria for early osteoarthritis of the knee. *Semin*
524 *Arthritis Rheum* **47**, 457-463 (2018).
525 16. Nevitt, M., Felson, D. & Lester, G. The osteoarthritis initiative. *Protocol for the cohort study*
526 **1**(2006).
527 17. Fromm, B.*, et al.* A Uniform System for the Annotation of Vertebrate microRNA Genes
528 and the Evolution of the Human microRNAome. *Annu Rev Genet* **49**, 213-242 (2015).
529 18. Riolo, G., Cantara, S., Marzocchi, C. & Ricci, C. miRNA targets: from prediction tools to
530 experimental validation. *Methods and protocols* **4**, 1 (2020).
531 19. Kuhn, D.E.*, et al.* Experimental validation of miRNA targets. *Methods* **44**, 47-54 (2008).
532 20. Pastrello, C.*, et al.* Osteoarthritis Data Integration Portal (OsteoDIP): a web-based gene
533 and non-coding RNA expression database. *Osteoarthritis and Cartilage Open* **4**, 100237
534 (2022).
535 21. Krämer, A., Green, J., Pollard Jr, J. & Tugendreich, S. Causal analysis approaches in
536 ingenuity pathway analysis. *Bioinformatics* **30**, 523-530 (2014).
537 22. Van Der Kraan, P.M. & Van Den Berg, W.B. Osteophytes: relevance and biology.
538 *Osteoarthritis and cartilage* **15**, 237-244 (2007).
539 23. Knights, C.B., Gentry, C. & Bevan, S. Partial medial meniscectomy produces osteoarthritis
540 pain-related behaviour in female C57BL/6 mice. *Pain* **153**, 281-292 (2012).
541 24. Vincent, T.L. Peripheral pain mechanisms in osteoarthritis. *Pain* **161**, S138-S146 (2020).

542 25. Lin, A.C., *et al.* Modulating hedgehog signaling can attenuate the severity of osteoarthritis.
543 *Nature Medicine* **15**, 1421-1425 (2009).
544 26. Lian, J.B. & Stein, G.S. Runx2/Cbfa1: a multifunctional regulator of bone formation. *Curr*
545 *Pharm Des* **9**, 2677-2685 (2003).
546 27. Smith, A.E., Sigurbjörnsdóttir, E.S., Steingrimsson, E. & Sigurbjörnsdóttir, S. Hedgehog
547 signalling in bone and osteoarthritis: the role of Smoothened and cholesterol. *The FEBS*
548 *journal* **290**, 3059-3075 (2023).
549 28. Ali, S.A., *et al.* Regulation of cholesterol homeostasis by hedgehog signaling in
550 osteoarthritic cartilage. *Arthritis & Rheumatology* **68**, 127-137 (2016).
551 29. Baghel, M., *et al.* Circulating microRNA profiles in early-stage osteoarthritis and
552 rheumatoid arthritis. *Scientific Reports* **15**, 27612 (2025).
553 30. Gao, F., *et al.* The human genome encodes a multitude of novel miRNAs. *Nucleic Acids*
554 *Res* **53**(2025).
555 31. Londin, E., *et al.* Analysis of 13 cell types reveals evidence for the expression of numerous
556 novel primate- and tissue-specific microRNAs. *Proc Natl Acad Sci U S A* **112**, E1106-1115
557 (2015).
558 32. Nishida, Y., *et al.* Serum Cartilage Oligomeric Matrix Protein Detects Early Osteoarthritis
559 in Patients With Anterior Cruciate Ligament Deficiency. *Arthroscopy* **38**, 873-878 (2022).
560 33. Singh, S., Jindal, D. & Khanna, R. Can serum MMP-3 diagnose early knee osteoarthritis?
561 *J Orthop* **38**, 42-46 (2023).
562 34. Füzéry, A.K., Levin, J., Chan, M.M. & Chan, D.W. Translation of proteomic biomarkers
563 into FDA approved cancer diagnostics: issues and challenges. *Clinical proteomics* **10**, 13
564 (2013).
565 35. Rocha, F.A.C. & Ali, S.A. Soluble biomarkers in osteoarthritis in 2022: year in review.
566 *Osteoarthritis Cartilage* **31**, 167-176 (2023).

567 36. Jones, T.L., *et al.* Osteoporosis, fracture, osteoarthritis & sarcopenia: A systematic review
568 of circulating microRNA association. *Bone* **152**, 116068 (2021).
569 37. Bauer, D., *et al.* Classification of osteoarthritis biomarkers: a proposed approach.
570 *Osteoarthritis and Cartilage* **14**, 723-727 (2006).
571 38. Donell, S. Subchondral bone remodelling in osteoarthritis. *EFORT Open Rev* **4**, 221-229
572 (2019).
573 39. Vicente, R., Noël, D., Pers, Y.M., Apparailly, F. & Jorgensen, C. Deregulation and
574 therapeutic potential of microRNAs in arthritic diseases. *Nat Rev Rheumatol* **12**, 211-220
575 (2016).
576 40. Ziemian, S.N., Witkowski, A.M., Wright, T.M., Otero, M. & van der Meulen, M.C.H. Early
577 inhibition of subchondral bone remodeling slows load-induced posttraumatic osteoarthritis
578 development in mice. *J Bone Miner Res* **36**, 2027-2038 (2021).
579 41. Crowe, N., *et al.* Detecting new microRNAs in human osteoarthritic chondrocytes identifies
580 miR-3085 as a human, chondrocyte-selective, microRNA. *Osteoarthritis Cartilage* **24**,
581 534-543 (2016).
582 42. Guo, Z., *et al.* Genome-wide survey of tissue-specific microRNA and transcription factor
583 regulatory networks in 12 tissues. *Sci Rep* **4**, 5150 (2014).
584 43. Lex, R.K., *et al.* GLI transcriptional repression is inert prior to Hedgehog pathway
585 activation. *Nat Commun* **13**, 808 (2022).
586 44. Xiao, W.F., Li, Y.S., Deng, A., Yang, Y.T. & He, M. Functional role of hedgehog pathway
587 in osteoarthritis. *Cell Biochem Funct* **38**, 122-129 (2020).
588 45. Seyhan, A.A. Trials and Tribulations of MicroRNA Therapeutics. *Int J Mol Sci* **25**(2024).
589 46. World Medical Association Declaration of Helsinki: ethical principles for medical research
590 involving human subjects. *Jama* **310**, 2191-2194 (2013).
591 47. Wilson, T., Kaur, N., Davis, J. & Ali, S.A. Tissue collection and RNA extraction from the
592 human osteoarthritic knee joint. *Journal of Visualized Experiments (JoVE)*, e62718 (2021).

593 48. Livak, K.J. & Schmittgen, T.D. Analysis of relative gene expression data using real-time
594 quantitative PCR and the 2− ΔΔCT method. *methods* **25**, 402-408 (2001).
595 49. Grimson, A.*, et al.* MicroRNA targeting specificity in mammals: determinants beyond seed
596 pairing. *Mol Cell* **27**, 91-105 (2007).
597 50. Lorenz, R.*, et al.* ViennaRNA Package 2.0. *Algorithms Mol Biol* **6**, 26 (2011).
598 51. Rauluseviciute, I.*, et al.* JASPAR 2024: 20th anniversary of the open-access database of
599 transcription factor binding profiles. *Nucleic acids research* **52**, D174-D182 (2024).
600 52. Pai, B.*, et al.* NMDA receptor-dependent regulation of miRNA expression and association
601 with Argonaute during LTP in vivo. *Front Cell Neurosci* **7**, 285 (2014).
602 53. Shima, W.N.*, et al.* Rapid growth and osteogenic differentiation of mesenchymal stem
603 cells isolated from human bone marrow. *Exp Ther Med* **9**, 2202-2206 (2015).
604 54. Gregory, C.A., Gunn, W.G., Peister, A. & Prockop, D.J. An Alizarin red-based assay of
605 mineralization by adherent cells in culture: comparison with cetylpyridinium chloride
606 extraction. *Analytical biochemistry* **329**, 77-84 (2004).
607 55. Glasson, S., Chambers, M., Van Den Berg, W. & Little, C. The OARSI histopathology
608 initiative–recommendations for histological assessments of osteoarthritis in the mouse.
609 *Osteoarthritis and cartilage* **18**, S17-S23 (2010).
610 56. Krenn, V.*, et al.* Grading of chronic synovitis--a histopathological grading system for
611 molecular and diagnostic pathology. *Pathol Res Pract* **198**, 317-325 (2002).
612 57. Armstrong, A.R., Carlson, C.S., Rendahl, A.K. & Loeser, R.F. Optimization of histologic
613 grading schemes in spontaneous and surgically-induced murine models of osteoarthritis.
614 *Osteoarthritis and cartilage* **29**, 536-546 (2021).

615

616

617

618 **Acknowledgements**

619 MB discloses support for this research from the Postdoctoral/Resident Fellowship awarded by the
620 Orland Bethel Family Musculoskeletal Research Center, University of Pittsburgh Department of
621 Orthopaedic Surgery, and Orthopaedic Research Society. We thank participants of the Henry
622 Ford Health OA Cohort for donating biospecimens.

623

624 **Author contributions**

625 MB, TGW, and SAA were involved in study conception and design. MB and TGW performed
626 experimental work and data acquisition. TB, JD, and VM contributed to the Henry Ford Health OA
627 Cohort. MB, TGW, and SAA performed data analysis, interpretation, and drafted the manuscript.
628 All authors contributed to manuscript revisions and approved the final version.

629

630 **Competing Interests**

631 SAA declares the following patent: Kapoor M, Ali SA, Gandhi R, & Appleton T. US Provisional
632 Patent Application No. 63/033,463. Circulating MicroRNAs in Knee Osteoarthritis and Uses
633 Thereof, filed on June 2, 2020. All other authors declare no conflicts of interest.

634

635

636

637

638

639

640

641

642

643

644 **Figure Legends**

645 **Figure 1. Circulating novel_miRNA_2 distinguishes early-stage knee OA.** A) Overview of the
646 approach used by Ali et al. (2020)[14] to identify four novel microRNAs prevalent in early-stage knee
647 OA plasma. Image created in BioRender. B) Relative plasma levels of novel_miRNA_2 in the
648 HFH OA Cohort. Values represent the fold-change relative to non-OA controls (n = 16/group).
649 Bars represent mean ± 95% confidence interval. *p < 0.05 as determined by one-way ANOVA
650 with Tukey's HSD post hoc test. C) Pearson correlation of plasma novel_miRNA_2 levels versus
651 Kellgren-Lawrence (KL) grade (n = 40). Data fitted from novel_miRNA_2 plasma levels relative to
652 a reference microRNA (miR-24-3p). Black line = fitted linear model. Grey shaded region = 95%
653 confidence interval. D) Area under the receiver operating characteristic curve (AUC) analysis
654 evaluating the accuracy of novel_miRNA_2 plasma levels in distinguishing early-stage knee OA
655 (EOA) from non-OA controls (blue line) and late-stage knee OA (LOA; red line). E) Multiple linear
656 regression analysis evaluating the association of covariates with plasma novel_miRNA_2 levels.
657 M = male, F = female, BMI = body mass index, 95% CI = confidence interval. Statistical
658 significance for regression coefficients determined by two-sided t-tests. P-values: B) p = 0.000
659 (Early Knee OA vs. Non-OA), p = 0.002 (Early Knee OA vs. Late Knee OA), p = 0.003 (Late Knee
660 OA vs. Non-OA).

661

662 **Figure 2. Novel_miRNA_2 functions as a canonical microRNA.** A) Overview of the putative
663 biogenesis of novel_miRNA_2. RISC = RNA-induced silencing complex. Image created in
664 BioRender. B) Predicted secondary structure of the novel_miRNA_2 precursor located in the
665 *ZNF773* host gene on human chromosome 19 (Chr19). Mature novel_miRNA_2 (highlighted
666 yellow) originates from the 5' arm of the precursor. Image created in BioRender. C) *ZNF773*, D)
667 pri-novel_miRNA_2, and E) mature novel_miRNA_2 levels in early- (n = 3-7) and late-stage (n =
668 7) knee OA tissues. Data represent fold-change values relative to the average levels in
669 corresponding late-stage knee OA tissues. Bars represent mean ± 95% confidence interval. *p <

670 0.05 as determined by two-sided Mann-Whitney U-test (*ZNF773*) or two-sided Welch's T-test (pri-
671 novel_miRNA_2 and novel_miRNA_2). "Bone" = subchondral bone, "FP" = infrapatellar fat pad,
672 "Cart" = articular cartilage, "Syn" = synovium. F) Overview of AGO2-RNA immunoprecipitation
673 assay in knee OA subchondral bone. Image created in BioRender. G) Relative enrichment of
674 novel_miRNA_2 and U6 small nuclear RNA negative control (snRNA) in IgG- or AGO2-bound
675 fractions as measured by RT-qPCR. Data represent fold-change values relative to the
676 corresponding IgG-bound fraction (n = 3). Bars represent mean ± 95% confidence. *p < 0.05 as
677 determined by two-sided Welch's T-test. P-values: C) p = 0.007 (Bone), p = 0.001 (FP), p = 0.067
678 (Cart), p = 0.035 (Syn). D) p = 0.000 (Bone), p = 0.005 (FP), p = 0.055 (Cart), p = 0.109 (Syn). E)
679 p = 0.018 (Bone), p = 0.018 (FP), p = 0.017 (Cart), p = 0.042 (Syn). G) p = 0.021
680 (novel_miRNA_2), p = 0.347 (U6 snRNA).
681
682 **Figure 3. Novel_miRNA_2 inhibits target genes in knee OA subchondral bone.** A) Strategy
683 to prioritize predicted novel_miRNA_2 target genes in OA. ∆G = Gibbs free energy. B) List of the
684 13 shortlisted target genes with features of their predicted novel_miRNA_2 binding sites, ranked
685 by predicted flanking region ∆G. C) RT-qPCR in knee OA subchondral bone transfected with
686 novel_miRNA_2 mimic or negative control (n = 5). Data represented relative to negative control-
687 treated tissues (dashed line). Bars represent mean ± 95% confidence interval. *p < 0.05 versus
688 matched negative control. D) Spectrophotometric quantification of Alizarin Red S staining (n = 6
689 technical replicates). Data represented relative to negative control-treated cells. Bars represent
690 mean ± 95% confidence interval. *p < 0.05. E) Representative images of MC3T3-E1 cells stained
691 with von Kossa or Alizarin Red S dyes to visualize mineralization following transfection with
692 novel_miRNA_2 mimic or negative control. Scale bars = 1 mm. All significance assessed by
693 paired two-sided Student's T-test. P-values: C) p = 0.000 (novel_miRNA_2), p = 0.007 (*ASPN*),
694 p = 0.031 (*RUNX2*), p = 0.040 (*ATRNL1*), p = 0.041 (*ADRA2A*), p = 0.031 (*SLC2A4*), p = 0.047
695 (*ITGA11*), p = 0.019 (*IL11*), p = 0.023 (*ALPL*), p = 0.041 (*MMP25*). D) p = 0.000.

696

697 **Figure 4. Novel_miRNA_2 has a protective effect in early-stage knee OA.** A) Overview of the
698 experimental design for mouse surgeries and novel_miRNA_2 mimic treatments. PMX = partial
699 medial meniscectomy. Sx = surgery. Tx = treatment. Image created in BioRender. B)
700 Representative images from *in situ* hybridization depicting localization of novel_miRNA_2 mimic
701 in mouse knee subchondral bone. Scale bars = 200 μm. Insets show magnified regions (scale
702 bars = 50 μm, arrows = positive signal). C) Representative coronal sections of mouse operated
703 knee, stained with Safranin-O. Scale bars = 1 mm. Insets show magnified regions (scale bars =
704 100 μm, arrows = examples of cartilage damage). D) OARSI scoring of PMX and sham mice
705 following novel_miRNA_2 mimic or control treatments (n = 5). Bars represent mean maximal
706 quadrant score ± 95% confidence interval. *p < 0.05. E) Representative coronal sections of mouse
707 operated knee demonstrating osteophyte burden. Scale bars = 250 μm. Brackets = approximate
708 osteophyte diameter. F) Osteophyte area in PMX and sham mice following novel_miRNA_2 mimic
709 or control treatments (n = 5). Datapoints represent the mean of the medial tibial and medial
710 femoral osteophyte area for each mouse. Bars represent the mean osteophyte area ± 95%
711 confidence interval, *p < 0.05. All significance assessed by two-sided Mann-Whitney U-test with
712 Benjamini-Hochberg multiple testing correction. P-values: D) p = 0.030 [novel_miRNA_2 mimic:
713 PMX (Early Tx) vs. PMX (Late Tx)], p = 0.016 [PMX (Early Tx): Negative control vs.
714 novel_miRNA_2 mimic]. F) p = 0.024 [novel_miRNA_2 mimic: PMX (Early Tx) vs. PMX (Late Tx)],
715 p = 0.032 [PMX (Early Tx): Negative control vs. novel_miRNA_2 mimic].

716

717 **Figure 5. Hedgehog (Hh) signaling may regulate novel_miRNA_2 levels in knee OA.** A) GLI
718 consensus binding motifs in the region 2.5 kb upstream of novel_miRNA_2 within *ZNF773*. Red
719 = positive strand, blue = negative strand. TSS = transcription start site. B) RT-qPCR in human
720 knee OA subchondral bone (n = 7/group). Data represent fold-change relative to late-stage knee
721 OA tissues. Bars represent mean ± 95% confidence interval. *p < 0.05 as determined by two-

722 sided Welch's T-test. C) Experimental design for Hh agonist (purmorphamine) treatments. Vehicle
723 = dimethyl sulfoxide (DMSO). Image created in BioRender. D) RT-qPCR in late-stage knee OA
724 subchondral bone explants following Hh agonist treatment (n = 5/group). Data represent fold-
725 change relative to paired vehicle (DMSO) control. Bars represent mean ± 95% confidence
726 interval. *p < 0.05. E) RT-qPCR in late-stage knee OA subchondral bone explants (n = 5/group)
727 following treatment with Hh agonist and concurrent novel_miRNA_2 mimic ("mimic"). Data
728 represent fold-change relative to Hh agonist alone. Bars represent mean ± 95% confidence
729 interval. *p < 0.05 as determined by two-sided paired Student's T-test. P-values: B) p = 0.000
730 (*GLI1*), p = 0.000 (*PTCH1*), p = 0.003 (*HHIP*), p = 0.001 (*RUNX2*). D) p = 0.030 (*GLI1*), p = 0.022
731 (*PTCH1*), p = 0.008 (*HHIP*), p = 0.013 (*ZNF773*), p = 0.015 (pri-novel_miRNA_2), p = 0.005
732 (novel_miRNA_2), p = 0.019 (*RUNX2*). E) p = 0.000 (novel_miRNA_2), p = 0.001 (*RUNX2*).
733
734 **Figure 6. Novel_miRNA_2 may mediate the effects of Hedgehog (Hh) signaling on *RUNX2***
735 **in knee OA subchondral bone**. In early-stage knee OA subchondral bone (left), reduced Hh
736 pathway activity coincides with elevated novel_miRNA_2 biogenesis and expression levels, which
737 can repress target genes such as *RUNX2*. In late-stage knee OA subchondral bone (right),
738 increased Hh pathway activity may suppress novel_miRNA_2 levels, potentially via GLI repressor
739 isoforms, and allow *RUNX2* to be elevated. When novel_miRNA_2 mimic is delivered beginning
740 in early stages of OA, its protective effects are maintained (bottom). Image created in BioRender.
741
742
743
744
745
746
747

748 **Supplemental Figures**

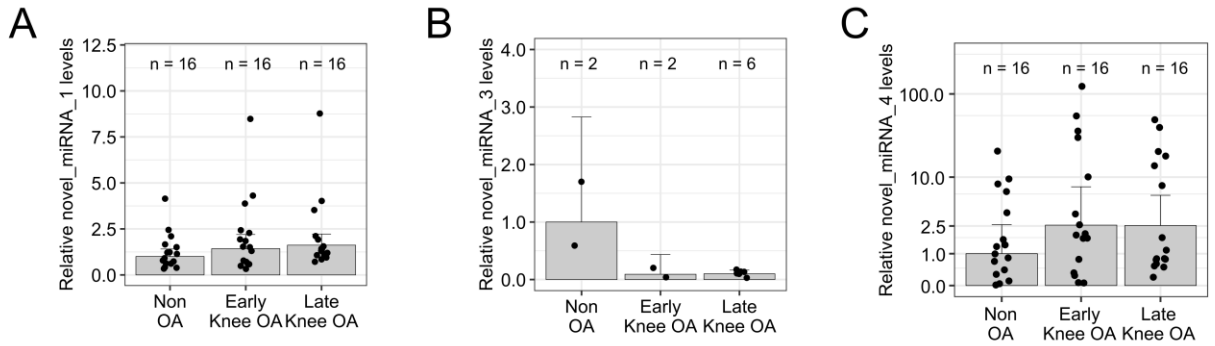

749

750 **Supplemental Figure 1. Novel microRNA levels in OA plasma.** RT-qPCR for (A)
751 novel_miRNA_1, (B) novel_miRNA_3, and (C) novel_miRNA_4 in the HFH OA Cohort. Data
752 represent the fold-change relative to non-OA controls. Bars represent mean ± 95% confidence
753 interval. Novel_miRNA_3 was not in the detectable range of RT-qPCR for 38/48 of the samples.
754 Significance not detected for any microRNA as assessed by Kruskal-Wallis test, p = 0.232
755 (novel_miRNA_1), p = N/A (novel_miRNA_3), p = 0.434 (novel_miRNA_4).

756

757

758

759

760

761

762

763

764

765

766

767

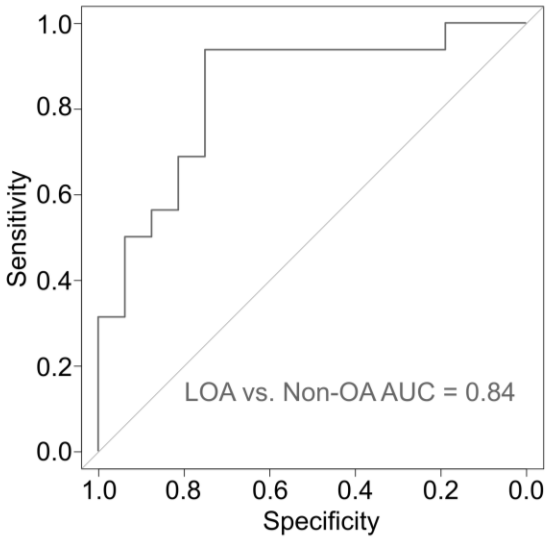

768

769 **Supplemental Figure 2. Accuracy of novel_miRNA_2 plasma levels in distinguishing late-**

770 **stage knee OA (LOA) from non-OA controls.** Area under the receiver operating characteristic

771 curve (AUC) analysis.

772

773

774

775

776

777

778

779

780

781

782

783

784

785

A

Mechanism name	Genes	IPA designation
Osteoarthritis	*ADRA2A, APOD, ASPN, ATRNL1, IL11, LEP, MMP25, PARD6G, RUNX2, SLC2A4*	Diseases and Functions
Hip or knee osteoarthritis	*ADRA2A, ASPN, IL11, RUNX2, SLC2A4*	Diseases and Functions
Osteoarthritis Pathway	*ADIPOQ, ALPL, ITGA11, LEP, RUNX2*	Canonical Pathway

B

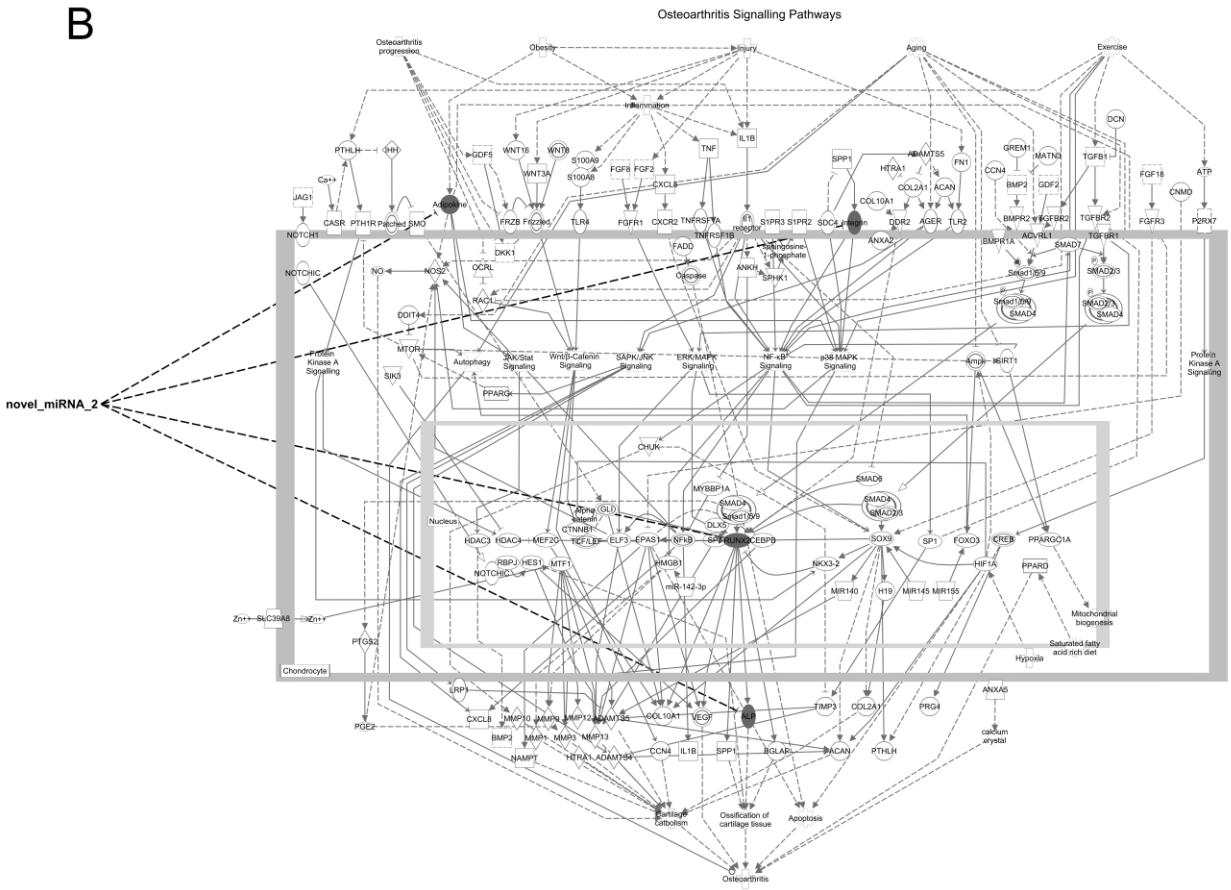

Supplemental Figure 3. Predicted novel_miRNA_2 target genes in curated 'Diseases and Functions' or 'Canonical Pathways' related to OA. A) Table of novel_miRNA_2 target genes stratified by Ingenuity Pathway Analysis (IPA) software core analysis results. B) 'Osteoarthritis Signaling Pathways' schematic generated by IPA showing predicted novel_miRNA_2 targets as shaded symbols.

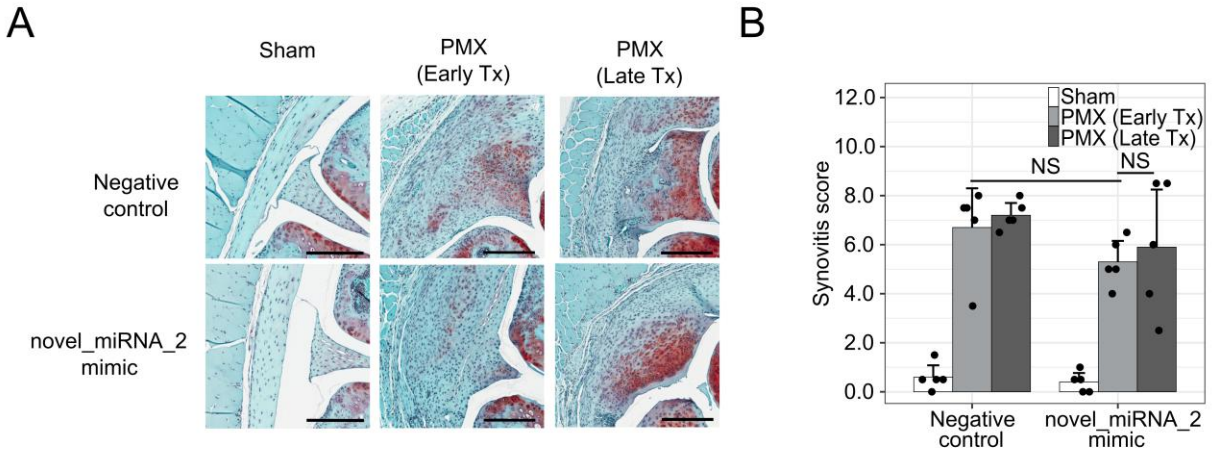

796

797 **Supplemental Figure 4. Male mice with knee OA show no change in synovitis**
798 **following novel_miRNA_2 mimic treatment.** A) Representative medial synovium from coronal
799 sections of mouse operated knees. Scale bars = 250μm. PMX = partial medial meniscectomy. Tx
800 = treatment. B) Krenn synovitis scoring in PMX and sham mice following novel_miRNA_2 mimic
801 or negative control treatments (n = 5). Bars represent mean synovitis score ± 95% confidence
802 interval. NS = not significant as determined by two-sided Mann-Whitney U-test. P-values: p =
803 0.141 [PMX (Early Tx): Negative control vs. novel_miRNA_2 mimic], p = 0.833 [novel_miRNA_2
804 mimic: PMX (Early Tx) vs. PMX (Late Tx)].

805

806

807

808

809

810

811

812

	Non OA	Early Knee OA	Late Knee OA	p-value
n (48 total)	16	16	16	-
Age (years) Mean (SD)	58.6 (11.2)	46.6 (12.2)	64.1 (8.3)	<0.01
Sex (female) n (%)	8 (50.0)	7 (43.8)	8 (50.0)	0.92
BMI (kg/m^2) Mean (SD)	27.0 (3.2)	27.6 (5.1)	31.9 (5.2)	<0.01
Race (white) n (%)	15 (93.8)	10 (62.5)	13 (81.2)	0.24

Supplemental Table 1. Clinicodemographic variables of plasma samples used from the HFH OA Cohort. n = sample size, SD = standard deviation, BMI = body mass index. Significance between groups assessed by one-way ANOVA for continuous variables and two-sided Chi-square test for categorical variables. P-values: p = 0.0001 (Age), p = 0.007 (BMI).

829

MicroRNA/gene symbol	Assay ID (TaqMan) or 5'–3' sequences (SYBR)
novel_miRNA_1	CSFXEVR
novel_miRNA_2	CTDJYDE
novel_miRNA_3	CTFVMKE
novel_miRNA_4	CTGZF6C
pri-novel_miRNA_2	APRWRTD
ZNF773	Hs00828818_m1
GAPDH (TaqMan)	Hs99999905_m1
ADRA2A	5'-CTTCTGGTTCGGCTACTGCAAC-3' - Forward 5'-GGAAACCTCACACGATCCGCTT-3' - Reverse
ADIPOQ	5'-CAGGCCGTGATGGCAGAGATG-3' - Forward 5'-GGTTTCACCGATGTCTCCCTTAG-3' - Reverse
ALPL	5'-GCTGTAAGGACATCGCCTACCA-3' - Forward 5'-CCTGGCTTTCTCGTCACTCTCA-3' - Reverse
APOD	5'-CAACTACTCACTAATGGAAAACGG-3' - Forward 5'-CTTGGCAGGCTCTGTGAGGTTA-3' - Reverse
ASPN	5'-CCACCAACTTTATTGGAGCTTCAC-3' - Forward 5'-CGTGGTATGTTAGCAAGACTCCC-3' - Reverse
ATRNL1	5'-AGATGATCGCCACCATACTGCC-3' - Forward 5'-CTGTTGAACCGACAGACCACGT-3' - Reverse
GLI1	5'-AGCCTTCAGCAATGCCAGTGAC-3' - Forward 5'-GTCAGGACCATGCACTGTCTTG-3' - Reverse
HHIP	5'-GCCATTCAGTAATGGTCCTTTGG-3' - Forward 5'-TGCCACTGCTTTGTCACAGGAC-3' - Reverse
IL11	5'-GGACCACAACCTGGATTCCCTG-3' - Forward 5'-AGTAGGTCCGCTCGCAGCCTT-3' - Reverse
ITGA11	5'-GCCTCCAGTATTTTGGCTGCAG-3' - Forward 5'-GCTCAAAGTGGAGGCTGGCATT-3' - Reverse
LEP	5'-GCTGTGCCCATCCAAAAAGTCC-3' - Forward 5'-CCCAGGAATGAAGTCCAAACCG-3' - Reverse
MMP25	5'-TGACAAGCCCACAAGGAAACCC-3' - Forward 5'-GATGGCGTCAAAATTGCCCTCAC-3' - Reverse
PARD6G	5'-GAGACCTGCTGCCCATCAACAA-3' - Forward 5'-CGCCGAGGCTGCCACGCTC-3' - Reverse
PTCH1	5'-GCTGCACTACTTCAGAGACTGG-3' - Forward 5'-CACCAGGAGTTTGTAGGCAAGG-3' - Reverse
RUNX2	5'-CCCAGTATGAGAGTAGGTGTCC-3' - Forward 5'-GGGTAAGACTGGTCATAGGACC-3' - Reverse
SLC2A4	5'-CCATCCTGATGACTGTGGCTCT-3' - Forward 5'-GCCACGATGAACCAAGGAATGG-3' - Reverse
GAPDH (SYBR)	5'-CATCACTGCCACCCAGAAGACTG-3' - Forward 5'-ATGCCAGTGAGCTTCCCGTTCAG-3' - Reverse

830 **Supplemental Table 2. List of probes and primers used for RT-qPCR experiments.**

831

832 **Figures**

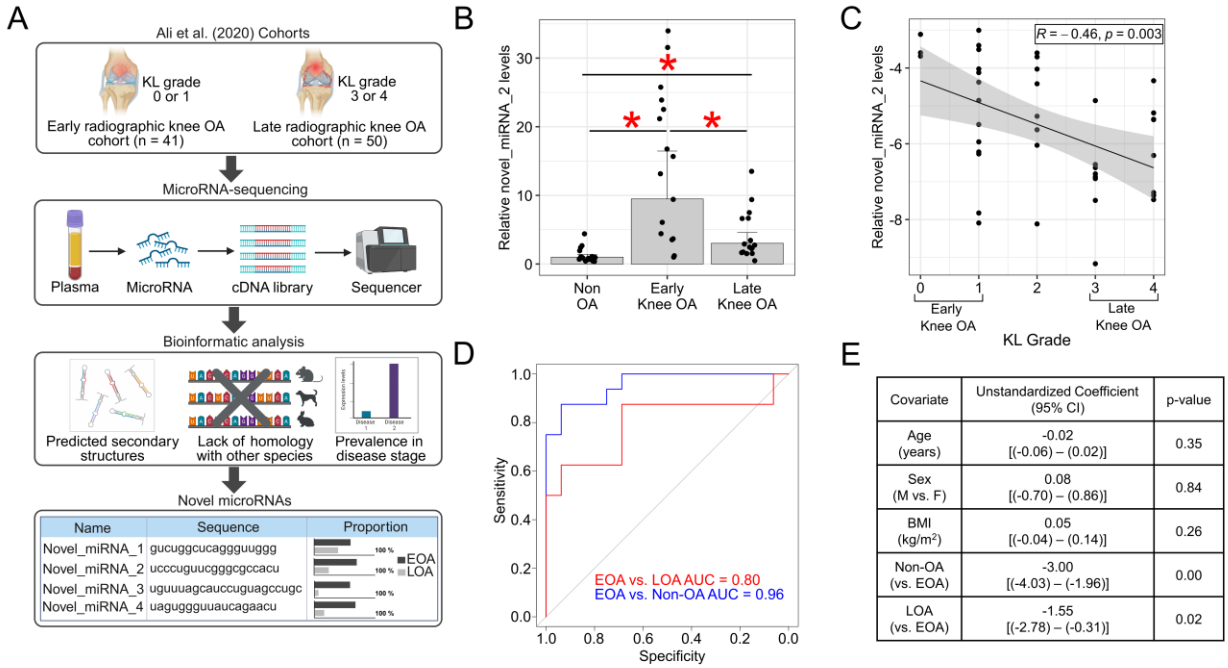

Covariate	Unstandardized Coefficient (95% CI)	p-value
Age (years)	-0.02 [(-0.06) – (0.02)]	0.35
Sex (M vs. F)	0.08 [(-0.70) – (0.86)]	0.84
BMI (kg/m^2)	0.05 [(-0.04) – (0.14)]	0.26
Non-OA (vs. EOA)	-3.00 [(-4.03) – (-1.96)]	0.00
LOA (vs. EOA)	-1.55 [(-2.78) – (-0.31)]	0.02

833

834 **Figure 1.**

835

836

837

838

839

840

841

842

843

844

845

846

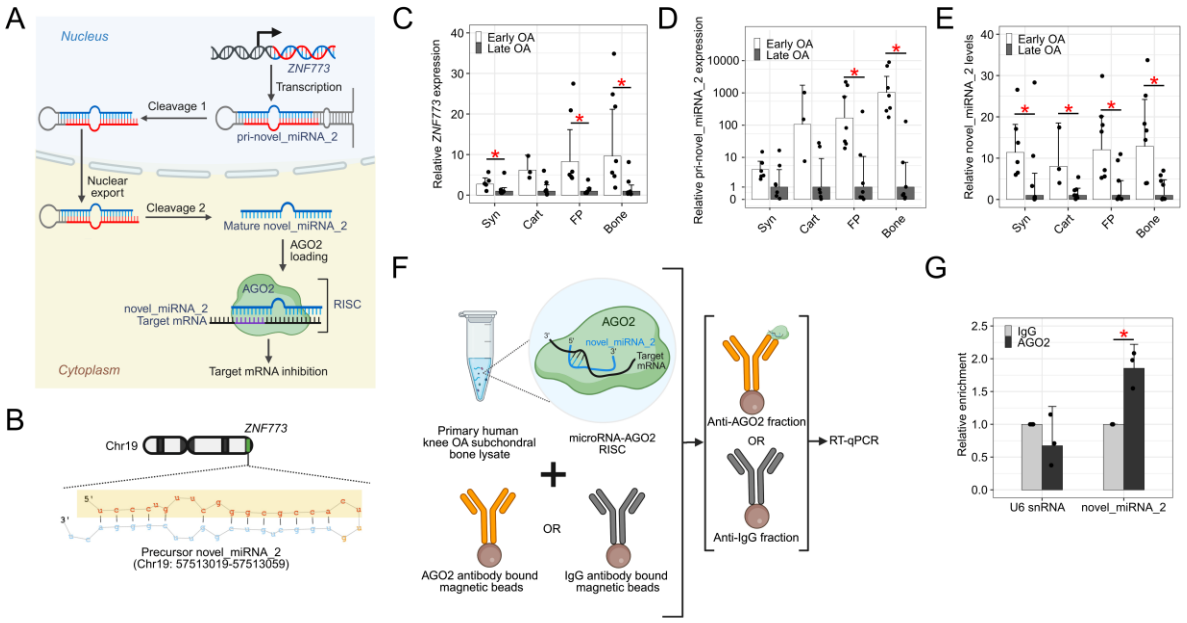
A
Nucleus
ZNF773
Transcription
Cleavage 1
pri-novel_miRNA_2
Nuclear export
Cleavage 2
Mature novel_miRNA_2
AGO2 loading
AGO2
novel_miRNA_2
Target mRNA
RISC
Cytoplasm
Target mRNA inhibition
B
Chr19
ZNF773
Precursor novel_miRNA_2
(Chr19: 57513019-57513059)
C
Early OA
Late OA
Relative ZNF773 expression
Syn
Cart
FP
Bone
D
Relative pri-novel_miRNA_2 expression
E
Relative novel_miRNA_2 levels
F
Primary human knee OA subchondral bone lysate
microRNA-AGO2 RISC
AGO2 antibody bound magnetic beads
OR
IgG antibody bound magnetic beads
Anti-AGO2 fraction
Anti-IgG fraction
RT-qPCR
G
IgG
AGO2
Relative enrichment
U6 snRNA
novel_miRNA_2

Figure 2.

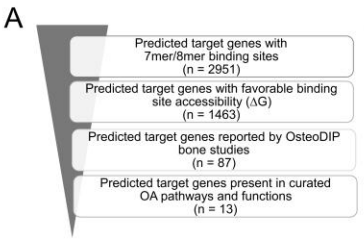

B

Gene symbol	Gene name	Molecule type	Binding site type (#)	Flanking ΔG (kcal/mol)	Non-flanking ΔG (kcal/mol)
APOD	Apolipoprotein D	Lipoprotein	7mer (1)	-0.7	-14.4
ASPN	Asporin	Proteoglycan	8mer (1)	-4.0	-8.5
RUNX2	Runt Related Transcription Factor 2	Transcription factor	7mer (1)	-7.2	-10.5
ATRNL1	Attractin-Like 1	Glycoprotein	8mer (1), 6mer (2)	-7.5	-10.8
PARD6G	Partitioning Defective 6 Homolog Gamma	Adapter protein	7mer (1)	-10.0	-13.0
ADRA2A	Adrenoceptor Alpha 2A	Adrenoceptor	7mer (1)	-10.2	-14.6
ADIPOQ	Adiponectin	Adipokine	7mer (2), 6mer (1)	-10.8	-11.2
SLC2A4	Solute Carrier Family 2 Member 4	Transporter	7mer (1)	-11.7	-16.4
ITGA11	Integrin Subunit Alpha 11	Alpha integrin	7mer (1), 6mer (2)	-11.9	-12.1
IL11	Interleukin 11	Cytokine	8mer (1), 6mer (1)	-13.1	-16.2
ALPL	Alkaline Phosphatase, Biomineralization Associated	Enzyme	7mer (1)	-13.3	-15.5
LEP	Leptin	Adipokine	7mer (1)	-14.4	-16.9
MMP25	Matrix Metallopeptidase 25	Enzyme	7mer (1)	-16.0	-21.6

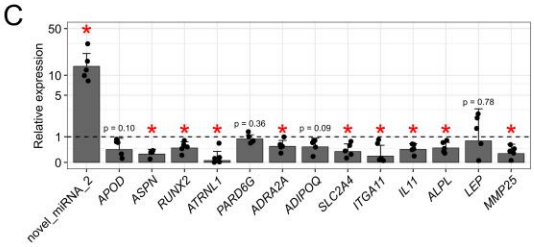

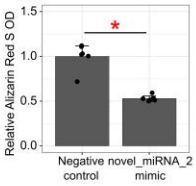

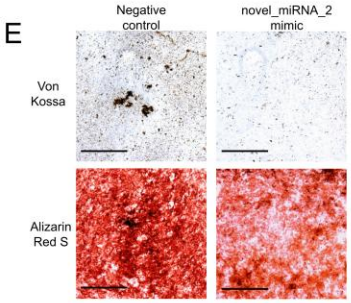

Figure 3.

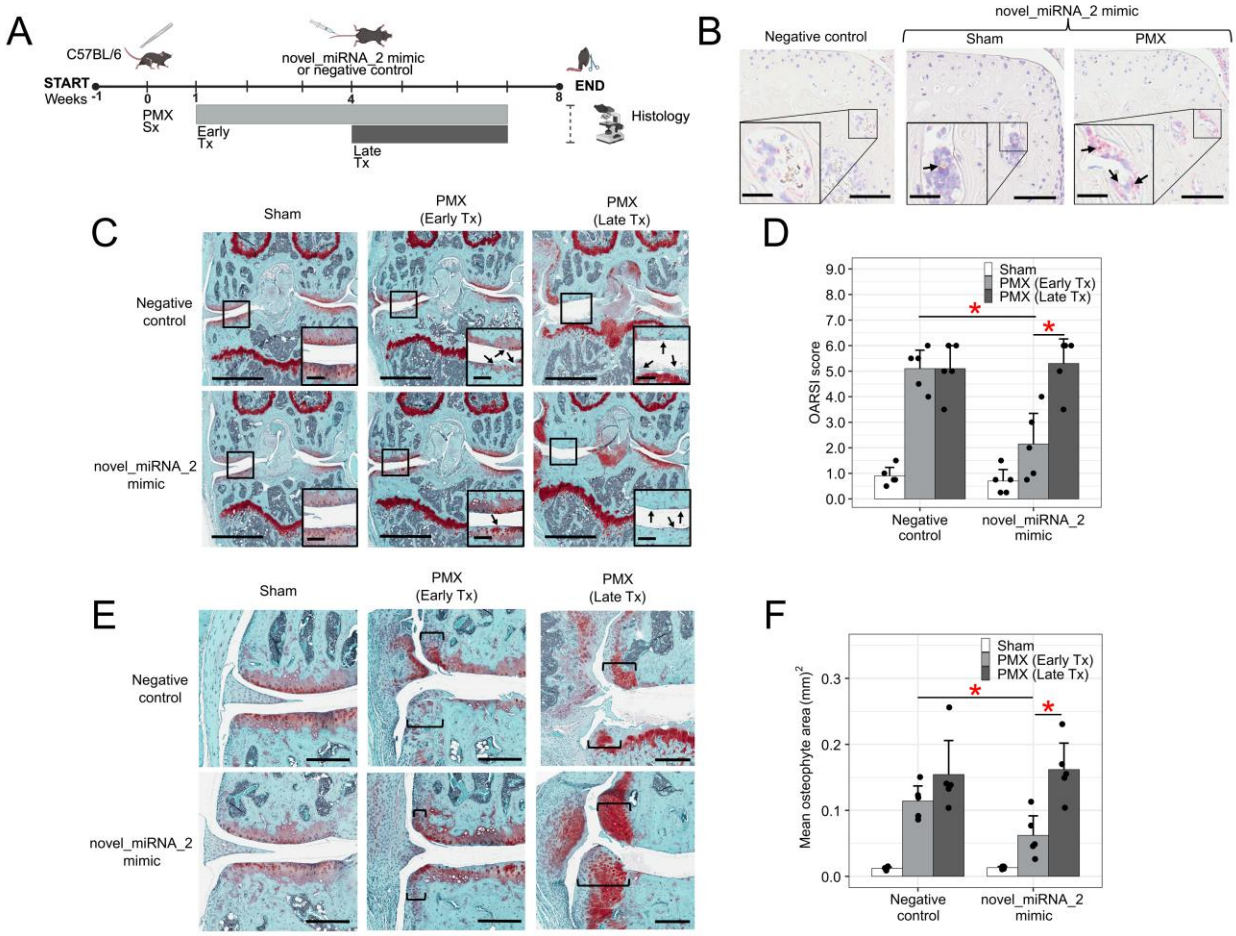
A
C57BL/6
novel_miRNA_2 mimic
or negative control
START
Weeks -1
0
1
4
8
END
PMX
Sx
Early
Tx
Late
Tx
Histology
B
novel_miRNA_2 mimic
Negative control
Sham
PMX
C
Sham
PMX
(Early Tx)
PMX
(Late Tx)
Negative
control
novel_miRNA_2
mimic
D
Sham
PMX (Early Tx)
PMX (Late Tx)
OARSI score
Negative
control
novel_miRNA_2
mimic
E
Sham
PMX
(Early Tx)
PMX
(Late Tx)
Negative
control
novel_miRNA_2
mimic
F
Sham
PMX (Early Tx)
PMX (Late Tx)
Mean osteophyte area (mm)^2
Negative
control
novel_miRNA_2
mimic

Figure 4.

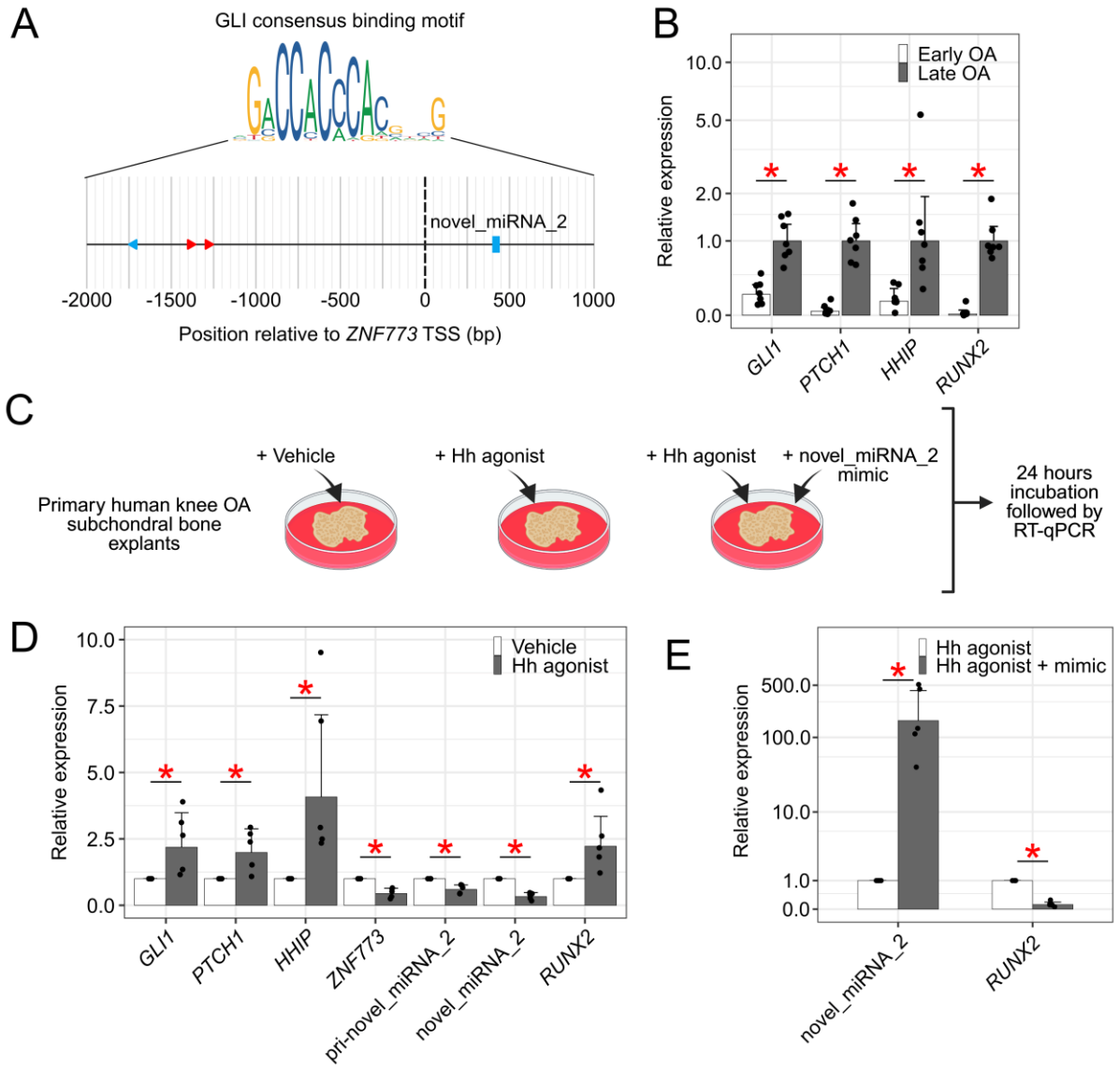
A
GLI consensus binding motif
novel_miRNA_2
-2000
-1500
-1000
-500
0
500
1000
Position relative to ZNF773 TSS (bp)
B
Early OA
Late OA
Relative expression
10.0
5.0
2.0
1.0
0.0
GLI1
PTCH1
HHIP
RUNX2
C
Primary human knee OA subchondral bone explants
+ Vehicle
+ Hh agonist
+ Hh agonist
+ novel_miRNA_2 mimic
24 hours incubation followed by RT-qPCR
D
Vehicle
Hh agonist
Relative expression
10.0
7.5
5.0
2.5
0.0
GLI1
PTCH1
HHIP
ZNF773
pri-novel_miRNA_2
novel_miRNA_2
RUNX2
E
Hh agonist
Hh agonist + mimic
Relative expression
500.0
100.0
10.0
1.0
0.0
novel_miRNA_2
RUNX2

Figure 5.

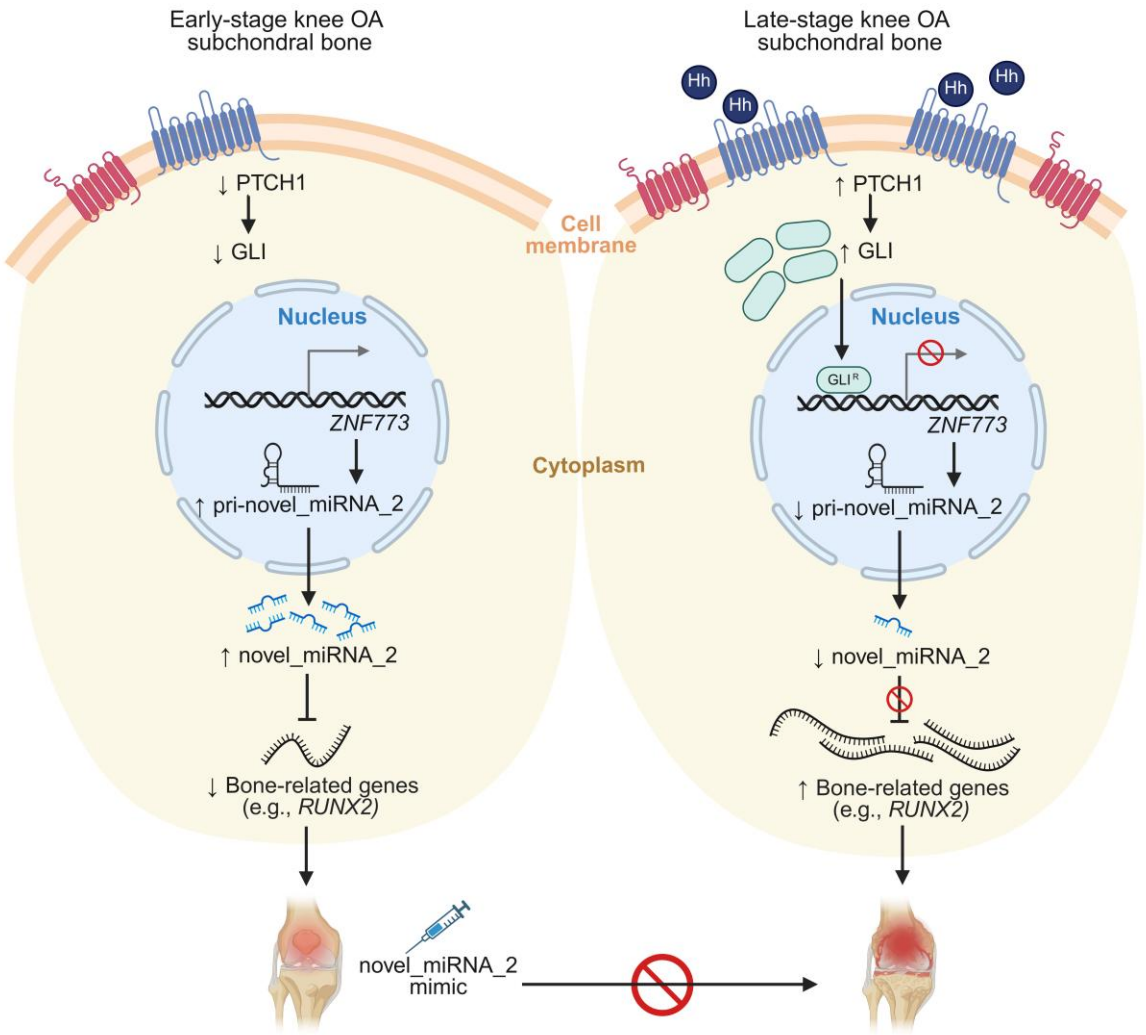
Early-stage knee OA
subchondral bone
Late-stage knee OA
subchondral bone
Hh
Hh
Hh
Hh
↓ PTCH1
↓ GLI
Cell
membrane
↑ PTCH1
↑ GLI
Nucleus
ZNF773
↑ pri-novel_miRNA_2
Cytoplasm
Nucleus
GLI^R
ZNF773
↓ pri-novel_miRNA_2
↑ novel_miRNA_2
↓ novel_miRNA_2
↓ Bone-related genes
(e.g., RUNX2)
↑ Bone-related genes
(e.g., RUNX2)
novel_miRNA_2
mimic

Figure 6.